

Geometric properties of two-dimensional $O(n)$ loop configurations

Chengxiang Ding¹, Xiaofeng Qian², Youjin Deng³, Wenan Guo¹ and Henk W.J. Blöte^{2,4}

¹ *Physics Department,
Beijing Normal University,
Beijing 100875, P.R.China*

² *Instituut Lorentz,
Universiteit Leiden, Postbus 9506,
2300 RA Leiden, The Netherlands*

³ *New York University, USA*

⁴ *Faculty of Applied Sciences,
Delft University of Technology,
P.O. Box 5046, 2600 GA Delft,
The Netherlands*

(Dated: March 11, 2018)

Abstract

We study the fractal geometry of $O(n)$ loop configurations in two dimensions by means of scaling and a Monte Carlo method, and compare the results with predictions based on the Coulomb gas technique. The Monte Carlo algorithm is applicable to models with noninteger n and uses local updates. Although these updates typically lead to nonlocal modifications of loop connectivities, the number of operations required per update is only of order one. The Monte Carlo algorithm is applied to the $O(n)$ model for several values of n , including noninteger ones. We thus determine scaling exponents that describe the fractal nature of $O(n)$ loops at criticality. The results of the numerical analysis agree with the theoretical predictions.

PACS numbers: 64.60.Ak, 64.60.Fr, 64.60.Kw, 75.10.Hk

I. INTRODUCTION

The $O(n)$ model consists of n -component spins $\vec{s}_i = (s_i^1, s_i^2, \dots, s_i^n)$ on a lattice, with isotropic, i.e., $O(n)$ invariant couplings. The common form of the reduced Hamiltonian of the $O(n)$ spin model is

$$H = -\frac{J}{k_B T} \sum_{\langle i,j \rangle} \vec{s}_i \cdot \vec{s}_j \quad (1)$$

where the indices i and j represent lattice sites, and the sum is over all nearest neighbor pairs; J is the coupling constant, k_B is Boltzmann's constant, and T is the temperature. Thus, the partition function of the model is

$$Z_{\text{spin}} = \int \prod_{\langle i,j \rangle} \exp\left(\frac{J}{k_B T} \vec{s}_i \cdot \vec{s}_j\right) \prod_k d\vec{s}_k \quad (2)$$

where the spins are normalized such that $\vec{s}_i \cdot \vec{s}_i = 1$. This model includes as special cases the Ising, the XY and the Heisenberg model, for $n = 1, 2$ and 3 , respectively.

In the high-temperature limit, the bond weight $w(\vec{s}_i \cdot \vec{s}_j)$ reduces in first order to $(1 + x \vec{s}_i \cdot \vec{s}_j)$ with $x = J/(k_B T)$. Thus the partition function takes the form

$$Z_{\text{spin}} = \int \prod_{\langle i,j \rangle} (1 + x \vec{s}_i \cdot \vec{s}_j) \prod_k d\vec{s}_k \quad (3)$$

The bond weight still satisfies the $O(n)$ symmetry implied by Eq. (1). According to the assumption of universality, the universality class of a phase transition is determined by only very few parameters including the symmetry of the spin-spin interactions. It is thus reasonable to expect [1] that the reduced Hamiltonian that corresponds with Eq. (3), namely $H = -\sum_{\langle i,j \rangle} \ln(1 + x \vec{s}_i \cdot \vec{s}_j)$ with $x = J/(k_B T)$ not necessarily small, still belongs to the $O(n)$ universality class in two dimensions.

The $O(n)$ model (3) on the honeycomb lattice can be mapped on the $O(n)$ loop model [2] on the same lattice, with a partition sum

$$Z_{\text{loop}} = \sum_G x^{N_b} n^{N_l} \quad (4)$$

where the graph G covers N_b bonds of the lattice, and consists of N_l closed, non-intersecting loops.

In the language of the $O(n)$ loop model, x is the weight of a bond visited by a loop, and n is the loop weight, and no longer restricted to be an integer.

The research of $O(n)$ models is a subject of a considerable history, in which a prominent place is occupied by the exact results [1] for the $O(n)$ loop model on the honeycomb lattice. These results include the critical points for $-2 \leq n \leq 2$, and the temperature and the magnetic exponent.

Also the geometric description of fluctuations at and near criticality has a long history, which goes back to the formulation of phase transitions in terms of the droplet model [3]. For the q -state Potts model (for a review, see Ref. 4), it was found that the fractal dimension of Kasteleyn-Fortuin (KF) clusters [5] is equal to the magnetic scaling exponent y_h . More generally, geometric Potts clusters can be defined by connecting neighboring, equal Potts spins by a bond percolation process. Several new critical exponents were found by Coulomb gas and other methods [6, 7, 8, 9]. These exponents describe the geometric properties and the renormalization flow of this model.

For the $O(n)$ loop model, the fractal dimension d_l of the critical loop gas has, to our knowledge, not yet been derived explicitly. However, a clue can be obtained from the relation [9, 11] between the exponents describing random clusters of the tricritical Potts model, and those describing Potts clusters in the critical Potts model. From the equivalence of the critical $O(n)$ model and the tricritical $q = n^2$ -state Potts model [1], one can thus associate the fractal dimension d_l of the critical $O(n)$ loop gas to the hull fractal dimension of critical Potts clusters. The latter dimension was conjectured by Vanderzande [10].

In the present paper, we focus on a fundamental non-thermodynamic scaling dimension behind the geometric properties of $O(n)$ loops which follows from the known correspondence with the Coulomb gas [16], and relate it to some exponents describing such properties. These exponents are exact and include the fractal dimension d_l of $O(n)$ loops at criticality. From a similar calculation, Duplantier and Saleur [12, 13] derived the fractal dimension d_a of the interior of these loops.

While theoretical predictions are available, thus far there is no numerical evidence in support of these, except for the Ising case $n = 1$ or $q = 2$ [11]. One of the reasons behind this situation may be that the $O(n)$ partition sum contains the number of loops. In the existing Monte Carlo algorithm for the loop model [14], the acceptance probability of a local update thus depends (for $n \neq 1$) on the change of the number of loops due to the Monte Carlo move. The determination of this number is a nonlocal task and requires a number of operations that increases algebraically with the system size L . Critical slowing down can

make this situation even worse, so that this way of simulation is restricted to rather small system sizes.

Until now, a sufficiently efficient Monte Carlo algorithm for the $O(n)$ loop model has not been described. Therefore, in this work, we develop a new Monte Carlo algorithm, which is applicable to models with noninteger $n > 1$, and uses local updates. Although these updates typically lead to nonlocal modifications of the loop connectivities, the number of operations required per update is only of order one, and essentially independent of the system size.

We then apply the algorithm to the critical $O(n)$ loop model and determine exponents of some geometric observables. The results agree with the theoretical predictions.

The outline of the rest of this paper is as follows. In Sec. II we show how a fundamental non-thermodynamic scaling dimension behind some geometric properties of $O(n)$ loops can be derived exactly from a mapping on the Coulomb gas, and how it relates to exponents describing some geometric observables. Section III introduces the Monte Carlo algorithm. In Sec. IV we apply the algorithm to the critical $O(n)$ loop model and determine exponents of some geometric observables.

II. COULOMB GAS DERIVATION AND SCALING FORMULAS

It is well known that geometric and fractal properties of $O(n)$ loops and various types of critical clusters can be analyzed by means of a mapping on the Coulomb gas [15, 16]. A number of exact scaling dimensions was obtained by this technique, see e.g., Refs. 8, 12, 13, 16, 17. Here we base ourselves on these analyses, which rely on a reformulation of correlation functions $g(r)$ in the model of interest in terms of the Coulomb gas. The dimensions $X(e, m)$ associated with such correlation functions are described by pairs of electric and magnetic charges, (e_0, e_r) and (m_0, m_r) , separated by a distance r :

$$X(e, m) = -\frac{e_0 e_r}{2g} - \frac{m_0 m_r g}{2} \quad (5)$$

where g is the coupling constant of the Coulomb gas. For the critical $O(n)$ model it is given by

$$g = 1 + \frac{1}{\pi} \arccos \frac{n}{2} \quad (6)$$

where we use a normalization that is in agreement with earlier literature but different from that used in Ref. 16 (our g is four times smaller, and the charges differ by a factor two such

that the $X(e, m)$ are the same).

Let us now consider the correlation function at criticality describing the probability that two lattice edges separated by a distance r are part of the same loop. It decays with an exponent $2X_l$ where X_l is the $O(n)$ loop scaling dimension. The exponent X_l is described by a pair of magnetic charges $m_0 = -m_r = 1$ and a pair of electric charges $e_0 = e_r = 1 - g$. This leads to

$$X_l = 1 - \frac{1}{2g} \quad (7)$$

This dimension X_l is the renormalization exponent behind geometrical and fractal properties of $O(n)$ loops, just as the renormalization exponents X_t and X_h determine the thermodynamic singularities.

In another application of the Coulomb gas technique we can explore corrections to scaling associated [8] with the exponent X_{2l} that describes the decay of the probability that two $O(n)$ loops collide in two points separated by a distance r . The value of this exponent is determined by electric charges as above and magnetic charges $m_0 = -m_r = 2$:

$$X_{2l} = 1 - \frac{1}{2g} + \frac{3g}{2} \quad (8)$$

This exponent becomes marginal at $n = 2$ and is thus expected to lead to poor convergence of finite-size data near $n = 2$.

The physical relevance of X_l can be demonstrated by means of scaling arguments. The probability $g_l(r)$ that two points at a distance r lie on the same loop is, as given above, $g_l(r) \simeq ar^{-2X_l}$. Let, at criticality, the fractal dimension of the loops be d_l . Thus, under a rescaling by a linear factor b , the length l of the loop decreases by a factor b^{d_l} , and its density increases by a factor b^{2-d_l} . This determines the correlation in the rescaled system as $g_l(r/b) \simeq ab^{4-2d_l}r^{-2X_l}$ which is, as specified above, to be compared with $g_l(r/b) \simeq ab^{2X_l}r^{-2X_l}$. It thus follows that the fractal dimension of loops is

$$d_l = 2 - X_l \quad (9)$$

Let $P_l(l)$ be the density of loops of length l . It is natural that, at criticality, $P_l(l)$ depends algebraically on l , with an exponent denoted as p_l :

$$P_l(l) \propto l^{p_l}. \quad (10)$$

Under a rescaling by a linear factor b , the loop density is affected for two reasons: first, the loops decrease in length by a factor $b^{d_l} = b^{2-X_l}$; and second, the density increases by a factor

b^2 because the volume is reduced. Consistency requires that $P_l(l)dl = b^{-2}P_l(lb^{2-X_l})d(lb^{2-X_l})$ or $P_l(l) = b^{-X_l}P_l(lb^{2-X_l})$. The requirement $P_l(l) \propto l^{-p_l}$ yields $l^{-p_l} = (lb^{2+X_l})^{-p_l}b^{-2+X_l-2}$. Matching the exponents shows that

$$p_l = 1 + \frac{2}{2 - X_l} \quad (11)$$

Since scaling implies that the divergence of the expectation value of the linear size of the largest loop goes as $(x_c - x)^{-\nu} = (x_c - x)^{-1/y_t}$ when the critical point is approached, and the actual length $l_{\max}(x)$ as expressed in lattice edges behaves as a power $2 - X_l$ of the linear size, it follows that the largest loop length diverges as

$$l_{\max}(x) \propto (x_c - x)^{(X_l-2)/y_t} \quad (12)$$

For $L \rightarrow \infty$ and $x > x_c$, there exists an infinite spanning loop. Under a rescaling by a linear scale factor b its density increases by a factor b^{X_l} while, as usual, the temperature field $t \propto x - x_c$ scales as $t \rightarrow t' = b^{y_t}t$. The fraction $s_l(x - x_c)$ of the edges covered by the spanning loop scales as $s_l(b^{y_t}(x_c - x)) = b^{X_l}s_l((x_c - x))$. The choice $b = (x_c - x)^{-1/y_t}$ leads to a constant on the left hand side of this equation, and after substitution in the right hand side, the scaling behavior follows as

$$s_l(x_c - x) \propto (x_c - x)^{X_l/y_t} \quad (13)$$

The finite-size dependence of the similar fraction s_L of a system with finite size L at criticality can simply be found by rescaling the system to a given size, say 1. This leads to

$$s_L \propto L^{-X_l} \quad (14)$$

Including a correction to scaling, we may modify this into

$$s_L = aL^{-X_l}(1 + bL^{y_i} + \dots) \quad (15)$$

where $y_i = 2 - X_{2l}$ is a candidate for the leading correction exponent [8], and a and b are unknown amplitudes.

In analogy with magnetic systems, a susceptibility-like quantity χ_l can be defined on the basis of the distribution of the loop sizes as

$$\chi_l \equiv \sum_{l=1}^{l_{\max}} P_l(l)l^2 \quad (16)$$

According to the aforementioned scaling behavior, the largest loop in a critical system of finite size L has a length scale $l_{\max} \propto L^{2-X_l}$. Thus

$$\chi_l(L) \propto \sum_{l=1}^{L^{2-X_l}} l^{2-p_l} \quad (17)$$

Substitution of $p_l = 1 + 2/(2 - X_l)$ yields

$$\chi_l(L) \propto L^{2-2X_l} \quad (18)$$

Again, we can include corrections to scaling

$$\chi_l(L) = cL^{2-2X_l}(1 + dL^{y_i} + \dots) \quad (19)$$

with y_i as mentioned above, and c and d are unknown constants.

Another correlation function of interest describes the probability that two sites on the dual triangular lattice separated by a distance r sit inside the same loop (i.e., not separated by any loop of the model). The exponent X_a describing the decay of this function at criticality was derived by Duplantier and Saleur [13] as $X_a = 1 - g/2 - 3/(8g)$. The fractal dimension of the interior of $O(n)$ loops is therefore $d_a = 2 - X_a = 1 + g/2 + 3/(8g)$. The area inside a loop does not include the area inside loops enclosed by that loop. The exponent X_a thus also determines the finite-size scaling of the spanning loop. We are therefore interested in the fraction s_a of the dual lattice sites that sit inside the spanning loop. Scaling indicates that this quantity is subject to the following finite-size behavior:

$$s_a(L) \propto L^{-X_a} \quad (20)$$

We furthermore define another susceptibility-like quantity χ_a on the basis of the distribution $P_a(a)$ of the area a (expressed in the number of enclosed sites of the dual lattice) of the interior of the loops as

$$\chi_a(L) \equiv L^{-2} \sum_a P_a(a) a^2 \quad (21)$$

which is expected to scale as

$$\chi_a(L) \propto L^{2-2X_a} \quad (22)$$

III. MONTE CARLO ALGORITHM

In the existing Monte Carlo algorithm for the loop model [14], the local updates require time-consuming nonlocal operations as explained above. To get rid of these we adopt the following procedure.

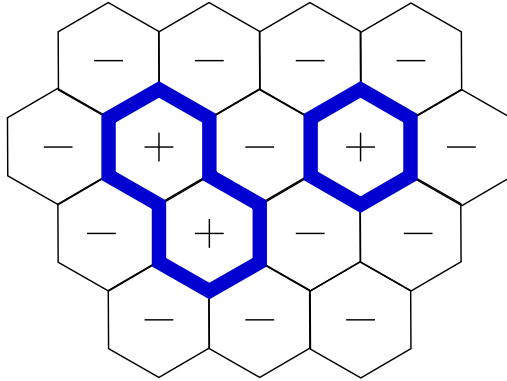


FIG. 1: Representation of a loop configuration with Ising spins

As a first step of such an algorithm for the simulation of the $O(n)$ loop model on the honeycomb lattice, we represent the loop configuration by means of Ising spins on the dual lattice, which is triangular. The loops are just the interfaces between neighboring spins of a different sign. We restrict ourselves to systems with periodic boundary conditions, so that the interfaces indeed form a system of closed, nonintersecting loops on the honeycomb lattice. This is illustrated in Fig. 1 using a loop configuration which consists of 2 loops and 16 bonds, shown as bold lines. This graph contributes a weight $x^{16}n^2$ to the partition function. The loops can of course be represented by two opposite Ising spin configuration, but this degeneracy has no further consequences for our line of argument.

We now show how one can update the loop configuration by means of local Metropolis-type updates of the Ising spins representing the loop configuration. It works only for $n \geq 1$. One step of importance sampling is realized by the following operations, which are to be repeated cyclically:

1. For each loop, assign its color to be either 'green' with probability $1/n$ or 'red' with the remaining probability $1 - 1/n$.
2. Randomly select an Ising spin on the dual lattice.
3. Check if the spin is adjacent to a red loop segment. If so, do nothing; if not, update the spin using the Metropolis probabilities, with Ising couplings K determined as $e^{-2K} = x$.
4. Repeat steps 2 and 3 until the number of update attempts is equal to the number of sites of the dual lattice.

5. Perform a sweep through the Ising system to find all loops.
6. Repeat steps 1 to 5 a fixed number $n_s - 1$ times.
7. Sample the data of interest from the loop configuration.

A Monte Carlo run consists of many of these cycles, each of which thus includes n_s Metropolis sweeps, new random assignments of loop colors, and the data sampling procedure. Each of these steps satisfies the conditions of detailed balance, so that the algorithm should indeed generate configurations in accordance with Boltzmann statistics. Tests confirm that the simulation results agree with those of the existing algorithm [14]. Since this algorithm assigns colors to the loops, we refer to it as "coloring algorithm".

IV. SIMULATION

With the help of the algorithm described above, we simulated the $O(n)$ model on the honeycomb lattice at the exactly known [1] critical points $x_c = (2 + (2 - n)^{1/2})^{-1/2}$ in order to check the theoretical predictions described in Sec. II.

We first applied our algorithm to the case $n = 1.5$, using 12 system sizes in the range $8 \leq L \leq 128$, where L is the linear size of the dual triangular lattice, and periodic boundary conditions.

For each system size, a run was executed with a length of 4×10^7 Monte Carlo cycles after equilibration of the system. Each cycle included $n_s = 5$ sweeps and loop formation steps, and one sampling as described above. Statistical errors were estimated by means of binning in 2000 partial results.

The data sampling included the density $P_l(l)$ of loops of length l . The results for the system of size $L = 128$ are shown in Fig. 2. It displays a substantial interval of algebraic decay, as described by Eq. (10).

The fractions s_l and s_a , and the susceptibility-like quantities χ_l and χ_a were also sampled. The finite-size dependence of these quantities at criticality is shown in Table I.

These quantities are well described by power laws as a function of the lattice size L for sufficiently large L . This is just as expected on the basis of finite-size scaling as expressed by Eqs. (14), (18), (20) and (22). This behavior is illustrated in Figs. 3, 4, 5 and 6.

TABLE I: numerical data for $s_l(L)$, $\chi_l(L)$ and $s_a(L)$, $\chi_a(L)$ for different system sizes L at the critical point of $O(n = 1.5)$ model

L	s_l	χ_l	s_a	χ_a
8	0.12907 (2)	0.8648 (1)	0.81028 (3)	2.166 (1)
16	0.08611 (2)	2.1984 (3)	0.76386 (5)	8.439 (6)
24	0.06785 (3)	3.4141 (6)	0.73829 (8)	18.39 (2)
32	0.05718 (3)	4.5578 (8)	0.72108 (9)	31.66 (5)
40	0.05006 (4)	5.6466 (11)	0.70812 (11)	48.15 (9)
48	0.04504 (4)	6.6993 (14)	0.69729 (13)	68.11 (14)
56	0.04107 (4)	7.7199 (23)	0.68869 (16)	90.80 (24)
64	0.03793 (4)	8.7142 (25)	0.68130 (15)	116.3 (3)
80	0.03324 (4)	10.635 (3)	0.66899 (19)	176.6 (6)
96	0.02987 (4)	12.477 (6)	0.65895 (22)	249.0 (10)
112	0.02723 (5)	14.273 (6)	0.65095 (26)	330.7 (14)
128	0.02513 (5)	16.027 (8)	0.6441 (3)	422.4 (23)

Using the nonlinear Levenberg-Marquardt least-squares algorithm, we fitted for the exponents and amplitudes according to the finite-size-scaling formulas including correction terms, as given in Eqs. (15), (19), (20) and (22). Thus we can numerically determine X_l , X_a , and thereby the fractal dimension d_l of the spanning loop, and the fractal dimension d_a of interior of the spanning loop. Comparing the residual χ^2 of the fits with the number of degrees of freedom, we find satisfactory fits including all system sizes $L \geq 8$. We obtain $X_l = 0.593$ (2) from the fit of $s_l(L)$ and $X_l = 0.595$ (2) from the fit of $\chi(L)$. These results are consistent with the theoretical value $X_l \approx 0.593513601$. The fit of $s_a(L)$ yields $X_a = 0.080$ (1). From the fit of $\chi_a(L)$, we obtain $2 - 2X_a = 1.84$ (1), or $X_a = 0.080$ (5). These results agree well with the theoretical prediction $X_a \approx 0.0801085234$.

In these fits, the correction-to-scaling exponent y_i was left free. The fits suggest that the exponent of the dominant correction to scaling does not assume the expected value $2 - X_{2l} = -0.43859$, but instead $y_i = -0.75 \pm 0.10$. On the other hand, we have also performed similar simulations of the $O(1)$ model at the critical point. The fractions s_l and s_a , and the susceptibility-like quantities χ_l, χ_a were sampled for several system sizes.

The results are shown in Tables II. Least-squares fit results agree well with the theoretical prediction, as listed in Table VI. For the $O(1)$ model, only the data for χ_l allowed a reasonably accurate estimate of the leading correction-to-scaling exponent. In this case, we find $y_i = -0.628(7)$, in a good agreement with the expected value $2 - X_{2l} = -0.625$. We thus have fixed y_i at this value in the other fits.

Furthermore we performed similar simulations of the $O(n)$ models with $n = \sqrt{2}$, $n = \sqrt{3}$ and $n = 2$ at their critical points as given in Ref. 1. The fractions s_l and s_a , and the susceptibility-like quantities χ_l, χ_a were sampled for several system sizes. The results are shown in Tables III, IV and V. Also these quantities appear to depend algebraically on the system size L , in agreement with the finite-size scaling equations (14), (18), (20) and (22).

TABLE II: Numerical data for $s_l(L)$, $\chi_l(L)$, $s_a(L)$ and $\chi_a(L)$ for several system sizes L at the critical point of the $O(n = 1)$ model.

L	s_l	χ_l	s_a	χ_a
8	0.09126 (2)	0.43532 (8)	0.88355 (2)	1.1563 (6)
16	0.06015 (2)	1.1859 (2)	0.85090 (5)	4.580 (5)
24	0.04678 (2)	1.8531 (3)	0.83257 (7)	10.108 (16)
32	0.03911 (2)	2.4658 (4)	0.81987 (9)	17.682 (39)
40	0.03405 (3)	3.0413 (6)	0.81015 (12)	27.27 (8)
48	0.03040 (3)	3.5901 (8)	0.80234 (14)	38.73 (13)
56	0.02754 (3)	4.1149 (12)	0.79617 (15)	51.68 (19)
64	0.02539 (4)	4.6235 (14)	0.79038 (20)	66.98 (32)
80	0.02214 (5)	5.5903 (24)	0.78077 (27)	104.0 (7)
96	0.01968 (5)	6.5121 (33)	0.77384 (28)	145.3 (11)
112	0.01781 (6)	7.4027 (42)	0.76799 (35)	193.0 (18)
128	0.01645 (6)	8.2442 (43)	0.76213 (42)	253.2 (26)

Using finite size scaling and the Levenberg-Marquardt algorithm, we determined the exponents X_l and X_a . The results are summarized in Table VI.

TABLE III: Numerical data for $s_l(L)$, $\chi_l(L)$, $s_a(L)$ and $\chi_a(L)$ for several system sizes L at the critical point of the $O(n = \sqrt{2})$ model.

L	s_l	χ_l	s_a	χ_a
8	0.12186 (2)	0.7813 (1)	0.82429 (3)	1.953 (1)
16	0.08104 (2)	1.9989 (3)	0.78004 (5)	7.651 (7)
24	0.06361 (3)	3.1027 (5)	0.75586 (8)	16.65 (2)
32	0.05358 (3)	4.1362 (7)	0.7392 (1)	28.81 (5)
40	0.04693 (4)	5.1183 (11)	0.7264 (1)	44.12 (9)
48	0.04206 (4)	6.0630 (16)	0.7164 (2)	62.14 (18)
56	0.03835 (5)	6.9786 (18)	0.7081 (2)	82.86 (22)
64	0.03536 (4)	7.8623 (22)	0.7011 (2)	106.5 (3)
80	0.03096 (5)	9.580 (4)	0.6890 (2)	162.4 (6)
96	0.02769 (5)	11.222 (5)	0.6800 (3)	227.0 (12)
112	0.02532 (6)	12.825 (7)	0.6716 (3)	304.4 (18)
128	0.02338 (6)	14.370 (9)	0.6649 (4)	390.7 (25)

V. DISCUSSION

The time-consuming character of simulations of loop models is due to the nonlocal character of the loops. We have reduced this problem by splitting the loop weight n in two parts, namely $n - 1$ and 1. Proper summation over both contributions is done by assigning color variables to the loops; a sum on all color variables is included in the partition sum. The algorithm treats these color variables as dynamical variables which are updated by the Monte Carlo process. The idea to use an additional color variable for each loop was already used in a context unrelated to Monte Carlo methods, e.g. in Ref. 18. The presence of loops of weight 1 in such a configuration then leads, at least locally, to a system that behaves precisely as an Ising configuration. Thus, the system may be locally updated by means of Metropolis-like Monte Carlo steps. Care should be taken to leave the loops of weight $n - 1$ unchanged, because it would violate the condition of detailed balance. The procedure given in Sec. III satisfies this constraint.

TABLE IV: Numerical data for $s_l(L)$, $\chi_l(L)$, $s_a(L)$ and $\chi_a(L)$ of the critical $O(n = \sqrt{3})$ model for several system sizes L .

L	s_l	χ_l	s_a	χ_a
8	0.15197 (2)	1.1247 (2)	0.76686 (3)	2.891 (1)
16	0.10286 (2)	2.8312 (3)	0.71434 (5)	11.150 (6)
24	0.08169 (3)	4.4245 (7)	0.68606 (6)	24.00 (2)
32	0.06929 (4)	5.9453 (12)	0.66677 (9)	41.16 (5)
40	0.06111 (4)	7.4130 (17)	0.6522 (1)	62.44 (9)
48	0.05500 (4)	8.8463 (23)	0.6408 (1)	87.2 1 (13)
56	0.05035 (4)	10.241 (3)	0.6314 (1)	115.7 (2)
64	0.04665 (4)	11.611 (4)	0.6233 (1)	148.0 (3)
80	0.04112 (5)	14.272 (6)	0.6098 (2)	223.7 (6)
96	0.03701 (4)	16.885 (7)	0.5993 (2)	311.0 (9)
112	0.03387 (4)	19.407 (9)	0.5906 (2)	411.4 (12)
128	0.03153 (5)	21.865 (11)	0.5824 (2)	531.2 (19)

The development of this coloring algorithm was motivated by the possibility to further explore the physics of $O(n)$ models. In the course of this work, we realized that it should be possible to construct an even more efficient algorithm of a ‘cluster’ nature. Algorithms of this type will be presented elsewhere [19]. The ‘coloring’ trick is only useful for $n > 1$. For $0 < n < 1$ the existing algorithm [14] is, although relatively inefficient, still applicable.

For the interpretation of the simulation results, it is relevant that we are using periodic boundary conditions, and that the mapping between loop and Ising configurations imposes a condition of ‘evenness’ on the loop configurations: a path spanning the periodic boundaries must have an even number of intersections with a loop. Therefore, the statistical ensemble generated by the algorithm does not coincide with that of Eq. (4). The difference is related to the boundary conditions and is expected to modify the finite-size behavior, but should vanish in the thermodynamic limit.

The present work is restricted to the ‘even’ loop configurations. It is, however, possible to simulate ‘odd’ loop configurations by introducing a ‘seam’ on the dual lattice, a vertical

TABLE V: Numerical data for $s_l(L)$, $\chi_l(L)$, $s_a(L)$ and $\chi_a(L)$ of the critical $O(n = 2)$ model for several system sizes L .

L	s_l	χ_l	s_a	χ_a
8	0.21534 (3)	1.7038 (3)	0.66465 (3)	5.082 (1)
16	0.15273 (2)	4.4449 (7)	0.60441 (3)	18.981 (6)
24	0.12479 (2)	7.2121 (11)	0.57283 (4)	39.965 (16)
32	0.10812 (2)	9.9856 (17)	0.55170 (4)	67.330 (29)
40	0.09674 (2)	12.762 (2)	0.53600 (5)	101.00 (5)
48	0.08832 (2)	15.544 (3)	0.52358 (5)	139.39 (7)
56	0.08177 (3)	18.328 (4)	0.51336 (6)	183.47 (11)
64	0.07650 (2)	21.106 (4)	0.50468 (5)	232.70 (14)
80	0.06844 (3)	26.676 (7)	0.49057 (7)	345.66 (30)
96	0.06243 (2)	32.251 (9)	0.47944 (6)	476.81 (37)
112	0.05783 (3)	37.828 (11)	0.47013 (7)	626.4 (5)
128	0.05410 (3)	43.392 (13)	0.46223 (7)	793.1 (7)
192	0.04418 (3)	65.680 (26)	0.43916 (10)	1620 (2)

TABLE VI: Results for the exponents X_l and X_a for five $O(n)$ models, as obtained from least-squares fits as described in the text.

n	X_l from s_l	X_l theory	$2 - 2X_l$ from χ_l	X_a from s_a	X_a theory	$2 - 2X_a$ from χ_a
1	0.625 (1)	5/8	0.73 (2)	0.0518 (3)	0.05208	1.89 (1)
$\sqrt{2}$	0.599 (1)	3/5	0.796 (5)	0.075 (1)	3/40	1.86 (1)
1.5	0.595 (3)	0.5935	0.810 (4)	0.080 (1)	0.08011	1.84 (1)
$\sqrt{3}$	0.571 (1)	0.5714	0.856 (1)	0.095 (1)	0.0952	1.81 (1)
2	0.4997 (3)	1/2	0.996 (5)	0.1249 (4)	1/8	1.747 (2)

column of horizontal antiferromagnetic Ising bonds spanning the system. For these antiferromagnetic bonds we use the rule that there is a loop segment if and only if the two associated dual spins are of the same sign. Horizontal and vertical seams can be introduced independently, as prescribed by the class of loop configurations that is to be sampled.

Acknowledgments

We wish to thank Prof. B. Nienhuis for many valuable discussions. This work was supported by the National Science Foundation of China under Grant #10105001, and by the Lorentz Fund (Leiden University).

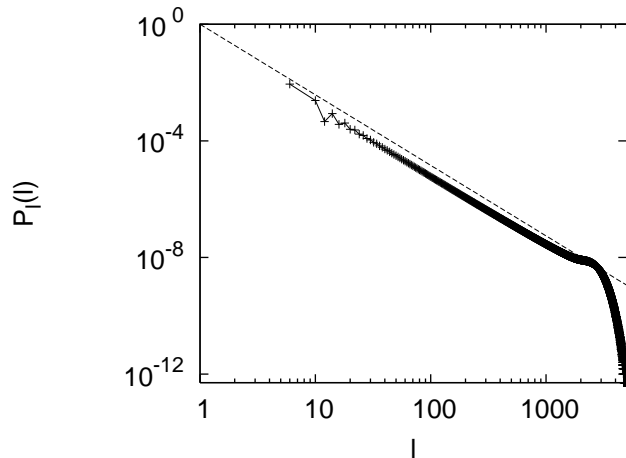


FIG. 2: Distribution P_l of loops of length l on logarithmic scales, for the critical $O(n)$ model with $n = 1.5$ and size $L = 128$. The dashed line shows a power law decay with exponent -2.42198318 , which is the theoretical asymptotic value for the infinite system.

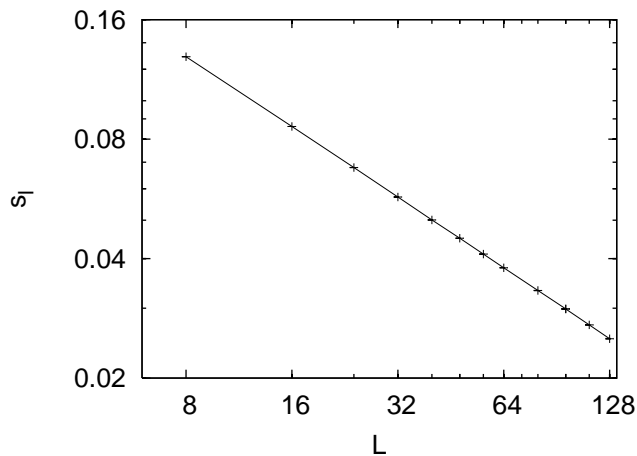


FIG. 3: Fraction s_l of lattice edges covered by the spanning loop, versus system size L for the critical $O(n)$ model with $n = 1.5$, on logarithmic scales. The curve is added as a guide to the eye, and estimated error bars are smaller than the size of the symbols.

[1] B. Nienhuis, Phys. Rev. Lett. **49**, 1062 (1982); J. Stat. Phys. **34**, 731 (1984).
 [2] E. Domany, D. Mukamel, B. Nienhuis and A. Schwimmer, Nucl. Phys. B **190**, 279 (1981).
 [3] M.E. Fisher, Physics (N.Y.) **3**, 25 (1967).
 [4] F.Y. Wu, Rev. Mod. Phys. **54**, 235 (1982).

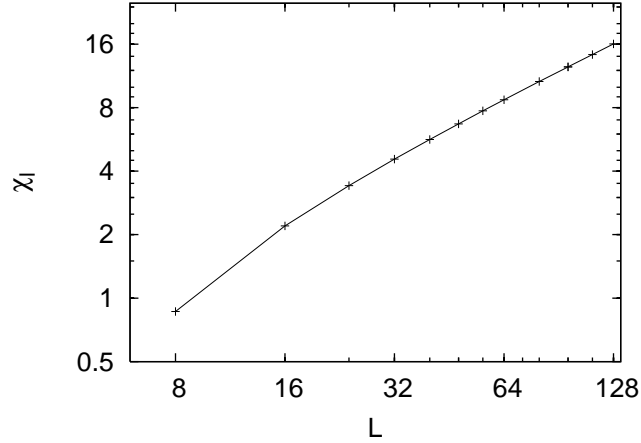


FIG. 4: Susceptibility-like quantity χ_L versus system size L for the critical $O(n)$ model with $n = 1.5$ on logarithmic scales. The curve is added as a guide to the eye, and estimated error bars are smaller than the size of the symbols.

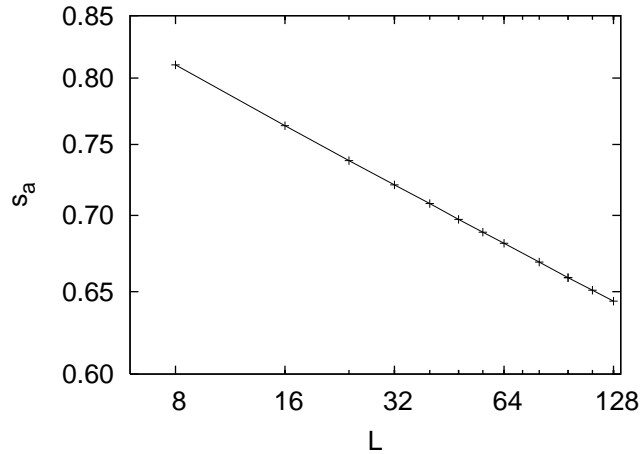


FIG. 5: Fraction s_a of the number of dual lattice sites inside the spanning loop, versus system size L for the critical $O(n)$ model with $n = 1.5$, on logarithmic scales. The curve is added as a guide to the eye, and estimated error bars are smaller than the size of the symbols.

- [5] P.W. Kasteleyn and C.M. Fortuin , J. Phys. Soc. Jpn. **46** (Suppl.), 11 (1969); C.M. Fortuin and P.W. Kasteleyn, Physica (Amsterdam) **57**, 536 (1972).
- [6] A. Coniglio and F. Peruggi, J. Phys. A **15**, 1873 (1982).
- [7] A. Coniglio, Phys. Rev. Lett. **62**, 3054 (1989).
- [8] H.W.J. Blöte, Y.M.M. Knops, and B. Nienhuis, Phys. Rev. Lett. **23**, 3440 (1992).
- [9] Y. Deng, H.W.J. Blöte and B. Nienhuis, Phys. Rev. E **69**, 026123 (2004).

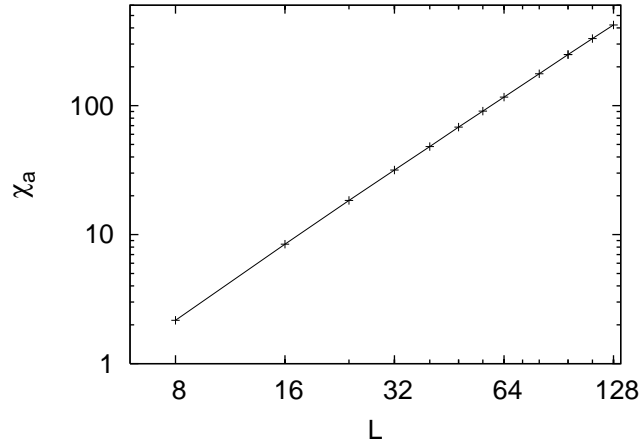


FIG. 6: Susceptibility-like quantity χ_a versus system size L for the critical $O(n)$ model with $n = 1.5$ on logarithmic scales. The curve is added as a guide to the eye, and estimated error bars are smaller than the size of the symbols.

- [10] C. Vanderzande, J. Phys. A **25**, L75(1992).
- [11] W. Janke and A.M.J. Schakel, Nucl. Phys. B **700**, 385 (2004).
- [12] H. Saleur and B. Duplantier, Phys. Rev. Lett. **58**, 2325 (1987).
- [13] B. Duplantier and H. Saleur, Phys. Rev. Lett. **63**, 2536 (1989).
- [14] W.A. Guo and H.W.J. Blöte, unpublished (2001).
- [15] L.P. Kadanoff, J. Phys. A **11**, 1399 (1978).
- [16] B. Nienhuis, in *Phase Transitions and Critical Phenomena*, Vol. **11**, edited by C. Domb and J.L. Lebowitz (Academic Press, London, 1987).
- [17] M.P.M. den Nijs, J. Phys. A **17**, L295 (1984).
- [18] H.W.J. Blöte and B. Nienhuis, J. Phys. A **22**, 1415 (1989).
- [19] Y. Deng, W.A. Guo, T. Garoni, A.D. Sokal and H.W.J. Blöte, to be published (2006).